

## THREE-DIMENSIONAL GAS DYNAMIC SIMULATION OF THE INTERACTION BETWEEN THE EXOPLANET WASP-12b AND ITS HOST STAR

D. BISIKALO<sup>1</sup>, P. KAYGORODOV<sup>1</sup>, D. IONOV<sup>1</sup>, V. SHEMATOVICH<sup>1</sup>, H. LAMMER<sup>2</sup>, AND L. FOSSATI<sup>3</sup>

<sup>1</sup> Institute of Astronomy, Russian Academy of Sciences, Moscow, Russia; [bisikalo@inasan.ru](mailto:bisikalo@inasan.ru)

<sup>2</sup> Space Research Institute, Austrian Academy of Sciences, Graz, Austria

<sup>3</sup> Argelander Institut für Astronomie der Universität Bonn, Bonn, Germany

Received 2012 September 6; accepted 2012 December 10; published 2013 January 21

### ABSTRACT

*Hubble Space Telescope* transit observations in the near-UV performed in 2009 made WASP-12b one of the most “mysterious” exoplanets; the system presents an early ingress, which can be explained by the presence of optically thick matter located ahead of the planet at a distance of  $\sim 4\text{--}5$  planet radii. This work follows previous attempts to explain this asymmetry with an exospheric outflow or a bow shock, induced by a planetary magnetic field, and provides a numerical solution of the early ingress, though we did not perform any radiative transfer calculation. We performed pure 3D gas dynamic simulations of the plasma interaction between WASP-12b and its host star and describe the flow pattern in the system. In particular, we show that the overfilling of the planet’s Roche lobe leads to a noticeable outflow from the upper atmosphere in the direction of the  $L_1$  and  $L_2$  points. Due to the conservation of the angular momentum, the flow to the  $L_1$  point is deflected in the direction of the planet’s orbital motion, while the flow toward  $L_2$  is deflected in the opposite direction, resulting in a non-axisymmetric envelope, surrounding the planet. The supersonic motion of the planet inside the stellar wind leads to the formation of a bow shock with a complex shape. The existence of the bow shock slows down the outflow through the  $L_1$  and  $L_2$  points, allowing us to consider a long-living flow structure that is in the steady state.

**Key words:** hydrodynamics – planet–star interactions – stars: individual: WASP-12

### 1. INTRODUCTION

WASP-12 is a late F-type main-sequence star ( $M_* = 1.35 M_\odot$ ,  $R_* = 1.6 R_\odot$ ,  $T_{\text{eff}} = 6250 \pm 100$  K,  $\log g = 4.2 \pm 0.2$ ; Fossati et al. 2010a) with a magnitude of  $V \sim 11^{\text{m}}6$ . The star is at a distance of about 400 pc from the Sun (Fossati et al. 2010a). The star hosts a transiting “hot Jupiter,” WASP-12b, with a mass of  $M_{\text{pl}} = 1.41 \pm 0.1 M_{\text{Jup}}$  and radius of  $R_{\text{pl}} = 1.74 \pm 0.09 R_{\text{Jup}}$  (Chan et al. 2011). WASP-12b revolves in a rather circular orbit (Campo et al. 2011) with a period of  $\sim 1.09$  days (Hebb et al. 2009) at a distance of 0.0229 AU ( $\sim 3$  stellar radii) from its host star.

WASP-12b was observed in 2009 in the near-UV with the Cosmic Origins Spectrograph (COS) on board *Hubble Space Telescope* (HST; Fossati et al. 2010b). The observed spectral range was 2540–2810 Å, divided into three bands of 40 Å each. Analysis of the COS light curves showed that the transit, in two of the three observed spectral regions, is considerably deeper than in the visible. Besides, an early ingress was also discovered. The HST data show that in the near-UV the transit starts approximately 50 minutes earlier than in the visible, meaning that ahead of the planet, at a distance of 4–5 planet radii, there is a region of absorbing matter.

So far, two explanations for this optically thick matter ahead of the planet have been proposed. The first explanation is based on mass transfer from the planet to the star (Lai et al. 2010; Li et al. 2010). Indeed, the distance of the center of the planet to the  $L_1$  point is only  $\sim 1.85 R_{\text{pl}}$ , and its upper atmosphere exceeds the Roche lobe.

The size of the collision-dominated atmosphere is limited by the exobase level  $R_{\text{ex}}$ , where the mean free path is equal to the atmosphere’s scale height. For WASP-12b’s atmosphere, which has an expected density at the base of the thermosphere of  $\rho_{\text{pl}} = 2.7 \times 10^{-14} \text{ g cm}^{-3}$  (see Section 2) and is heated by the stellar EUV radiation to a temperature of  $T_{\text{pl}} = 10^4$  K, the

exobase would expand beyond the Roche-lobe distance. Using standard physics of binary stars (see, e.g., Pringle & Wade 1985; Savonije 1979), to estimate how much the upper atmosphere overfills the Roche lobe, one can calculate the volume Roche radius  $R_{L_1}$ , obtaining  $\sim 1.37 R_{\text{pl}}$  and the degree of overfilling  $\Delta R/R_{L_1} = (R_{\text{ex}} - R_{L_1})/R_{L_1} \approx 0.13$ . Such a large degree of overfilling leads to a powerful outflow of material through the  $L_1$  and  $L_2$  points. The natural result of this outflow is the formation of an accretion disk surrounding the star, as for close binaries, where the flow structure is well studied, both analytically (see, e.g., Lubow & Shu 1975) and numerically (see, e.g., Bisikalo et al. 2003; Bisikalo & Fridman 2008; Zhilkin et al. 2012).

If the accretion disk is axisymmetric, it does not produce any effect on the transit shape. However, in the region where the stream interacts with the disk an observable extended shock wave forms (Boyarchuk et al. 2002; Bisikalo et al. 2003). This hypothesis was used by Lai et al. (2010), who supposed that the stream from  $L_1$  itself and/or the region of the stream–disk interaction can cause the early ingress. Although the idea is reasonable, a more detailed analysis shows that, with such a large degree of Roche-lobe overfilling, the lifetime of the planet atmosphere would be very short. In accordance with equations used in the theory of close binaries (see, e.g., Pringle & Wade 1985), the mass-loss rate is defined as

$$\dot{M}/M = (\Delta R/R)^3 \sqrt{\frac{GM}{R^3}}. \quad (1)$$

Using this equation and assuming a total mass of the WASP-12b’s atmosphere of  $1.41 M_{\text{Jup}}$ , we find that the lifetime of the atmosphere is no longer than several years. Accounting for the adjustment of the mass-loss rate with time, one can then more accurately estimate the lifetime of the outflowing atmosphere. Let us assume that the temperature of the thermosphere is constant, which is a reasonable assumption as WASP-12 is an inactive star (Fossati et al. 2010a). In this case,

the mass decrease of a gas giant planet leads to an increase of the Roche-lobe overfilling and consequently an increase of the mass-loss rate. As a matter of fact, for a gas giant planet, Equation (1) gives an estimate of the maximum planet lifetime. On the other hand, for a planet with a rocky core the mass of its atmosphere is just a small fraction of the total mass; therefore, one can assume that the size of the Roche lobe will be constant, independently of the atmosphere-loss rate. Hence, the part of the atmosphere that lies above the Roche lobe will flow out till the atmosphere itself becomes smaller than the Roche lobe, arresting the mass loss. In this way, for rocky planets one can use Equation (1) to obtain a reasonable estimate of the period of time in which the planet is actively losing mass. In other words, if the overfilling is high, the lifetime of the atmosphere will be short for any kind of planet, hence a small chance to observe it. Therefore, the hypothesis proposed by Li et al. (2010) and Lai et al. (2010) most likely does not allow an adequate explanation of the processes ongoing in the WASP-12 system. Nevertheless, this probability is not zero; it is indeed quite possible that for systems where the dynamic pressure of the wind is small the scenario proposed by Lai et al. (2010) is realistic. To some extent our work is a further development of this idea.

The second possible explanation is the presence of an optically thick bow shock region ahead of the planet, which possesses a proper magnetic field (Vidotto et al. 2010, 2011). This interpretation is based on the fact that the planet orbits with a supersonic velocity inside the stellar wind, forming a bow shock at a distance of  $\sim 4\text{--}5 R_{\text{pl}}$  ahead of the planet. Llama et al. (2011) performed radiative transfer calculations based on the Vidotto et al. model, showing that multiple shock configurations would fit the near-UV light curve, hence the need of further observations to constrain the model parameters.

Ionov et al. (2012) adopted a model similar to that of Vidotto et al. (2010) but assumed that the planet does not possess any magnetic field. In this case, the bow shock forms immediately at the level of the upper atmosphere. Although the authors were able to qualitatively model the light curve, the shock results to be at a distance significantly different from the observed one. The distance between the contact discontinuity and the center of the planet can be defined analytically considering the dynamic pressure balance from both sides of the contact discontinuity (Baranov & Krasnobaev 1977). For the considered case, this distance should not be greater than  $\sim 1.88 R_{\text{pl}}$  and the wave front should be located at  $\sim 2.23 R_{\text{pl}}$  from its center (Verigin et al. 2003), half of that indicated by the observations (see Lai et al. 2010). It is important to note that both bow shock models (Ionov et al. 2012; Vidotto et al. 2010) do not account for the presence of the outflowing atmosphere. In the presence of an overfilling Roche lobe the balance equations should take into account the dynamic and thermal pressure of the outflowing atmospheric gas. In this way, the positions of the bow shock and contact discontinuity will be defined by the gas properties. Vidotto et al. (2010) showed that the thermal pressure is negligible for a barometric distribution of the atmospheric gas. In the case instead of an outflowing atmosphere, the gas from the vicinity of the  $L_1$  point will form a stream with a slowly decreasing density, hence increasing the importance of the thermal pressure. More importantly, the stream from the  $L_1$  point accelerates in the gravitational field of the star, increasing its radial velocity as  $\sqrt{r}$ . As a consequence, the dynamic pressure of the stream will increase ( $\sim r$ ), while the importance of the magnetic field will decrease as  $r^{-3}$  ( $B^2 \sim r^{-6}$ ). This means that for an outflowing

atmosphere the role of the stream in the solution should be extremely relevant.

The aim of this study is the application of a 3D gas dynamic model to the gaseous envelope of WASP-12b, in order to provide an alternative explanation of the observed early ingress. This work will be followed by a more comprehensive study describing the sensitivity of the results on the assumption and presenting comparisons between the model and the available observations. The work is organized as follows. In Section 2, we describe our model and the assumed input parameters; in Section 3, we present the results of the numerical simulations; and in Section 4, the main results are discussed.

## 2. MODEL DESCRIPTION

The atmospheric parameters of WASP-12b are not well known; therefore, we assume an isothermal upper atmosphere with a temperature, which is defined by the host star's deposition of X-ray and ultraviolet energy and is similar to that obtained for other hot Jupiters:  $T_{\text{pl}} = 10^4$  K (Yelle 2004; Koskinen et al. 2012). Note that the assumed temperature of the thermosphere does not correspond to the equilibrium temperature, which is about 2500 K (Hebb et al. 2009), but to that of the lower thermosphere, which is close to the visual radius and is heated by the stellar EUV radiation (Yelle 2004; Koskinen et al. 2012).

We do not include stellar irradiation in the model, because this will affect just the boundary temperature value. In our simulation, we attempt to recover the presence of an early ingress at the observed distance, by changing the boundary conditions to obtain a solution where the stream from the  $L_1$  point is stopped by the stellar wind at the observed distance. On the other hand, the influence of the boundary temperature on the solution is rather important, because it defines the density of the atmospheric gas at the  $L_1$  point. This is a key parameter because it is used to gather the Roche-lobe overfilling and the power of the stream from the  $L_1$  point; this consequently defines the solution. We plan to include a more accurate description of the irradiation in a future work.

We estimated the density of the lower thermosphere considering that the optical depth along the line of sight is  $\tau = n_{\text{pl}} \times l_{\text{pl}} \times k_{\text{pl}} = 1$ . Here, the distance  $l_{\text{pl}}$  corresponds to the path followed by the line of sight through the spherical layer [ $R_{\text{pl}} - (R_{\text{pl}} + H_{\text{pl}})$ ], where  $H_{\text{pl}}$  is the scale height. To avoid uncertainties due to the calculation of the opacities  $k_{\text{pl}}$ , we assume that the atmosphere of WASP-12b is hydrogen dominated, similarly to what Vidal-Madjar et al. (2003) considered for HD 209458b, for which the number density at the photometric radius is  $\sim 2 \times 10^{10} \text{ cm}^{-3}$  (Murray-Clay et al. 2009). Taking into account that WASP-12b is  $\sim 2$  times heavier and  $\sim 1.6$  times larger (radius) than HD 209458b, we estimated the hydrogen number density at the photometric radius as  $n_{\text{pl}} \approx 1.6 \times 10^{10} \text{ cm}^{-3}$ , corresponding to a density of  $\approx 2.7 \times 10^{-14} \text{ g cm}^{-3}$ . We defined the obtained density at the photometric radius and the corresponding exobase at  $1.55 R_{\text{pl}}$ . For comparison, Lai et al. (2010) define the density at the 1 bar level and their exobase at  $1.59 R_{\text{pl}}$ , in agreement with our approach.

We consider a system configuration, comparable to a binary system, consisting of the star with  $M_* = 1.35 M_{\odot}$  and WASP-12b with mass  $M_{\text{pl}} = 1.3 \times 10^{-3} M_{\odot}$ . Following the observations, we assume that the components of this binary system, having an orbital separation  $A = 4.9 R_{\odot}$ , move in a circular

orbit with a period  $P_{\text{orb}} = 26^h$ . The linear velocity of the planet in this system is  $230 \text{ km s}^{-1}$ .

The flow is described by a 3D system of gravitational gas dynamic equations closed by the equation of state of a perfect neutral monatomic gas. In this model we neglect the non-adiabatic processes of radiative heating and cooling. An analysis of our solution shows that the density of the envelope is rather high, so everywhere in the envelope the Knudsen number<sup>4</sup> is  $< 1$ . In the important regions of the solution (along the streams from the  $L_1$  and  $L_2$  points) the Knudsen number is always  $< 0.1$ , allowing us to assume that a gas dynamic approach is valid for the problem considered here.

In our model we use the gas dynamic equations, with the assumption that the planetary magnetic field is small. Indeed, the synchronization of hot Jupiters occurs within a few Myr (e.g., Showman & Guillot 2002, and references therein), while the age of the star is about 2 Gyr (Chan et al. 2011); hence, the planet should be tidally locked and therefore its magnetic field should be weak. There are certainly various further hypotheses for the formation of magnetic fields in gas giants (e.g., induced fields), but all of them do imply the presence of fields, which most likely would not protect the expanding upper atmosphere, especially in this case where the star is inactive (Fossati et al. 2010a). The presence of the large value of the magnetic field also contradicts the observations and stellar wind interaction models, which reproduce the observed  $\text{Ly}\alpha$  absorption spectra obtained during transits of hot Jupiters (e.g., Ekenbäck et al. 2010; Lammer et al. 2011).

To solve the system of gas dynamic equations, we use a Roe–Osher TVD scheme of a high-approximation order with the Einfeldt modification. This numerical method allows one to study flows with a significant density contrast. Further details of the numerical model can be found in Boyarchuk et al. (2002) and Bisikalo et al. (2003).

Calculations have been performed in a rotating coordinate frame where the force field can be described by the Roche potential

$$\Phi = -\frac{GM_*}{\sqrt{x^2 + y^2 + z^2}} - \frac{GM_{\text{pl}}}{\sqrt{(x - A)^2 + y^2 + z^2}} - \frac{1}{2}\Omega^2 \left[ \left( x - A \frac{M_{\text{pl}}}{M_* + M_{\text{pl}}} \right)^2 + y^2 \right], \quad (2)$$

where  $\Omega$  is the angular velocity of the system's rotation.

The origin of the coordinate system is at the center of the star; the  $X$ -axis is directed to the planet; the  $Z$ -axis coincides with the rotation axis of the system and is perpendicular to the orbital plane; the  $Y$ -axis finalizes the right-handed system. The calculations have been performed in a rectangular homogeneous grid. The size of the calculation domain is  $(25 \times 20 \times 10) R_{\text{pl}}$ , and the grid resolution is  $464 \times 363 \times 182$  cells. The accepted size of the cell of  $0.05 R_{\text{pl}}$  allows the investigation of all main flow pattern features in the planet's vicinity.

The boundary conditions have been set as follows. The upper atmosphere is assumed to be isothermal ( $T_{\text{pl}} = 10^4 \text{ K}$ ) and in hydrostatic equilibrium, i.e., the gas velocity in the upper atmosphere is zero. At the level  $r = R_{\text{pl}}$ , we set the value of the density at the visual radius equal to  $2.7 \times 10^{-14} \text{ g cm}^{-3}$ . At the

initial conditions, the density of the planet upper atmosphere was defined according to the barometric formula from the adopted boundary conditions till the distance where the density becomes less than the wind density. Outside this region the computational domain was filled by gas of stellar wind. We treated the stellar wind as done by Vidotto et al. (2010). The particle number density in the stellar wind has been set equal to  $5 \times 10^6 \text{ cm}^{-3}$  (Vidotto et al. 2010). The stellar wind parameters proper of WASP-12 are unknown; therefore, we used that of the solar wind. Namely, the temperature of the wind has been set equal to that of the Sun at the corresponding distance from the star,  $T = 10^6 \text{ K}$  (Withbroe 1988). The velocity of the wind is assumed to be  $100 \text{ km s}^{-1}$ , corresponding to the velocity of the solar wind at the distance of WASP-12b to the host star (Withbroe 1988). As the wind acceleration mechanism is still an open question, in the model we imply the existence of a wind acceleration mechanism that works similarly to light pressure. To take this into account, we modify the expression for the Roche potential, given in Equation (2), as follows:

$$\Phi = -\Gamma \cdot \frac{GM_*}{\sqrt{x^2 + y^2 + z^2}} - \frac{GM_{\text{pl}}}{\sqrt{(x - A)^2 + y^2 + z^2}} - \frac{1}{2}\Omega^2 \left[ \left( x - A \frac{M_{\text{pl}}}{M_* + M_{\text{pl}}} \right)^2 + y^2 \right],$$

where the  $\Gamma$  coefficient is used to account for the stellar wind acceleration and is set to 0 in the regions filled with wind matter and 1 in the rest of the calculation domain. This allows us to avoid the non-physical wind deceleration due to stellar gravity. The proper stellar wind velocity is subsonic with a Mach number  $M = 0.85$ . However, taking into account the supersonic orbital motion of the planet ( $M = 1.97$ ), the total velocity of the planet with respect to the stellar wind is indeed supersonic with the rather large Mach number of  $M = 2.14$ .

### 3. THE STRUCTURE OF THE PLANET GASEOUS ENVELOPE

The general morphology of the flow is shown in Figure 1, indicating the density distribution and velocity vectors in the planet's envelope. The planet is depicted by the filled circle and moves counterclockwise. The solid yellow lines denote the flow lines starting from the gas of the stellar wind. The Roche lobe, depicted by the white solid line, and Lagrangian points  $L_1$  and  $L_2$  are also shown.

Considering the density distribution shown in Figure 1, we notice that the planet's envelope has a non-spherical complex shape. In addition to the upper atmosphere itself, one can see flows toward the  $L_1$  and  $L_2$  points. According to the conservation of angular momentum, these streams are deflected in the direction of the planet's motion and against it, respectively. The supersonic motion of the planet and the presence of the stellar wind lead to the formation of a bow shock oriented according to the total vector of the wind material velocity with respect to the planet. The location of the shock and contact discontinuity can be easily determined from variations in the flow lines. It turns out that the head-on collision point is located on the gas stream from the  $L_1$  point. The distance between the planet center and the head-on collision point, as projected onto the stellar limb, is  $\sim 4.5$  planet radii, in agreement with the estimation by Lai et al. (2010), who derived the position of the early ingress at  $\sim 3.2$  planet radii, from the planet surface.

<sup>4</sup> The Knudsen number is defined as  $\text{Kn} = \lambda/H$ , where  $\lambda$  is the mean free path, equal to  $1/(n \times \sigma)$ , where  $n$  is the number density and  $\sigma$  is the cross section,  $\sigma = 10^{-15} \text{ cm}^2$ , and  $H$  is a typical scale of the solution  $H = n/(dn/dr)$ .



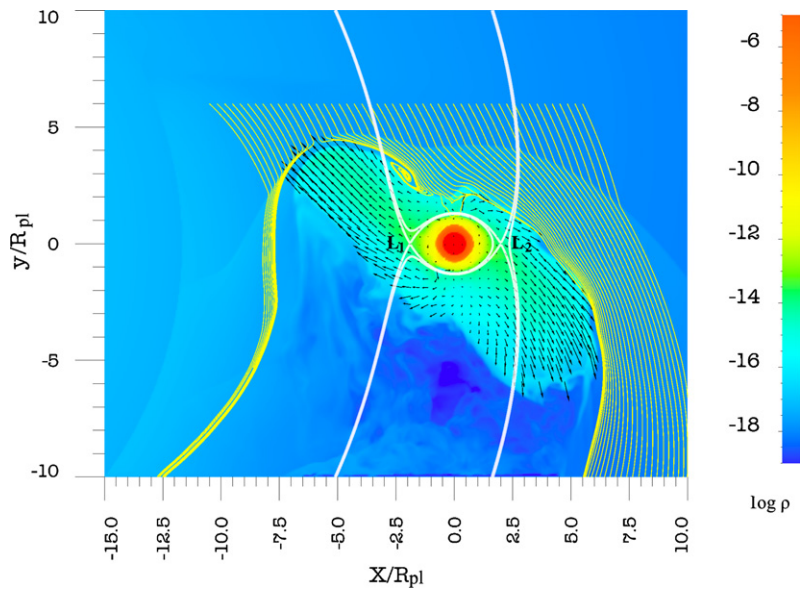


**Figure 1.** Density distribution and velocity vectors in the envelope of WASP-12b. The planet is depicted by the filled circle and moves counterclockwise. The solid yellow lines denote the flow lines starting in the gas of the stellar wind. The white solid lines denote the Roche equipotentials passing through the Lagrangian points  $L_1$  and  $L_2$ .

Both shock and contact discontinuity have complex shapes. The asymmetric shape of the planet envelope, the upper atmosphere itself, and two flows/prominences from  $L_1$  and  $L_2$  lead to the formation of a distinguishable double-peaked shock. The head-on collision point is at the peak of the “prominence” in the direction of  $L_1$ . However, when moving closer to the planet, we see that the shock bends due to the presence of the planetary atmosphere and shifts farther from the planet, leading to the formation of the second “hump” in the shock. It is noticeable that the matter’s flow, moving to the planet from the head-on collision point, undergoes strong disturbance when it gets into the cavity between the two humps in the shock waves. In particular, vortices form in this cavity. This effect smooths the contact discontinuity, mixing the matter of the stellar wind and upper atmosphere.

The flows toward the  $L_1$  and  $L_2$  points extend far away from the planet’s Roche lobe. Formally, the planet loses its atmosphere and, according to Equation (1), the lifetime of the atmosphere is not longer than a few years. However, in our simulation the envelope is in a quasi-stationary regime, i.e., it is almost enclosed. The dynamic pressure of the stellar wind and flow, caused by the orbital motion of the planet, breaks the propagation of the streams from the  $L_1$  and  $L_2$  points, limiting the gaseous envelope of the planet by the bow shock and contact discontinuity.

Let us consider the problem of the system closure in detail. From the physical point of view, the material that has left the planet’s exosphere through the vicinity of the  $L_1$  point should follow a certain trajectory determined by the balance of three forces: the force of inertia, gravity forces, and the gradient of gas pressure. We can neglect the gravity of the planet out of its Roche lobe; hence, the gas motion can be considered as that falling in the gravity field of the star. The stream is deflected by the Coriolis force. However, at moderate distances from the  $L_1$  point we can estimate the radial velocity of matter using the difference between the values of the potential energy at the point of our interest and the  $L_1$  point

$$v^2 \approx \Phi(L_1) - \Phi(\mathbf{r}), \quad (3)$$

where  $\Phi(\mathbf{r})$  is the Roche potential at the point with the radius vector  $\mathbf{r}$  and  $L_1$  is the radius vector of the inner Lagrangian point. With the motion in the gravity field of the star, the velocity of the stream grows. However, at the same time the wind density also grows in accordance with

$$\rho_w = \rho_{w0} \left( \frac{A}{|\mathbf{r}|} \right)^2. \quad (4)$$

It results that eventually the dynamic pressures of the stream  $\rho_s v^2$  and wind  $\rho_w v_w^2$  become equal and the radial motion of the stream ends. We only need to estimate at what distance this is happening and if this distance is in agreement with the observations.

According to ballistic analysis (Lubow & Shu 1975), the stream, moving in a binary system, is deflected from the line connecting the centers of mass of the star and planet at an angle of  $\sim 20^\circ$ . The dynamic influence of the wind should increase this angle, and, as follows from the results of the numerical simulations (see Figure 1), the angle grows up to  $\sim 40^\circ$ . For the location of the shock wave to correspond to the observed one ( $Y_w \approx 5 R_{pl}$  from the center), the radial motion of the stream should stop at a distance of  $X_w = -5 R_{pl} \tan 40^\circ \approx -6 R_{pl}$  from the  $L_1$  point. We can therefore write the following equation, setting the equilibrium between the dynamic pressures of the stream and wind (as done by Vidotto et al. (2010), but for an atmosphere with a magnetic field) and Equations (3) and (4):

$$\rho_{L_1} (\Phi(L_1) - \Phi(\mathbf{r})) = \rho_{w0} \left( \frac{A}{|\mathbf{r}|} \right)^2 v_w^2. \quad (5)$$

Solving this equation, we find analytically the density at the  $L_1$  point whose value allows us to stop the shock wave at the observed distance from the planet. Substituting the known value of  $\mathbf{r}$  (from the observations) into Equation (5), we obtain  $\rho_{L_1} \approx 1 \times 10^{-17} \text{ g cm}^{-3}$ , corresponding to a number density of  $n_{L_1} \approx 6 \times 10^6 \text{ cm}^{-3}$ . The obtained value is  $\sim 18$  times less than that at the  $L_1$  point, given by the barometric formula<sup>5</sup> where

<sup>5</sup> When determining this value, we assumed that the density is constant over the whole surface of the Roche lobe and is equal to the value found for the shortest distance from the planet to the lobe.

$\rho_{\text{pl}} = 2.7 \times 10^{-14} \text{ g cm}^{-3}$ . In the gas dynamic simulation, the stream stopped at the observed distance with the density value  $\rho_{\text{pl}} \approx 1.35 \times 10^{-15}$ , which is  $\sim 20$  times less than the boundary density, estimated using the planet's photometric radius. In our analysis we omitted the effects of the stream gas heating due to the bow shock's radiation, and we can state that the analytical estimates are in good agreement with the results of the numerical simulations.

The numerical simulations presented in this work allow us to simulate the formation of an enclosed and steady-state gaseous envelope surrounding "hot Jupiters" that exceed the planet's Roche lobe, such as WASP-12b. We should note one more important property of the described model of the planet's envelope. Observations indicate (Fossati et al. 2010b) that the eclipse in the spectral bands where the early ingress has been observed is two times deeper than the eclipse of the planet itself (3.2% versus 1.7%). The possible explanation for this effect can also be the formation of a bow shock. Indeed, the motion of the planet inside the stellar wind is significantly supersonic, and the formed bow shock is much hotter than the planet upper atmosphere. The heating of the gaseous envelope including the stream from the  $L_1$  point leads to the excitation and broadening of additional lines in the UV bands. According to Vidal-Madjar et al. (2004) and Ben-Jaffel (2007), the depth of the transit at some spectral bands strongly depends on its width and presence of strong spectral lines. The larger the equivalent width of the lines in a certain band, the deeper the transit in this band. Therefore, the additional heating of the planet envelope can lead to the observed effect of a stronger absorption in the near-UV bands.

#### 4. CONCLUSIONS

Using 3D numerical simulations, we investigated the flow pattern in the vicinity of the exoplanet WASP-12b, which is overfilling its Roche lobe. Taking into account that the planet is tidally locked, we assumed no (or negligible) surface magnetic field and consider the pure gas dynamic solution. In this work, we study the flow structure of the forming gaseous envelope surrounding the planet, without including any radiative transfer calculation. The obtained solution depends strongly on the stellar wind parameters, which we assumed close to solar.

Our results indicate the following:

1. Because the planet's upper atmosphere overfills its Roche lobe, WASP-12b's envelope has a complex non-spherical shape. In addition to the central part of the spherical upper atmosphere, two "prominences," directed to the  $L_1$  and  $L_2$  Lagrangian points, develop in the system. These streams leave the planet and are deflected in the direction of the orbital motion and against it. Under the action of the dynamic pressure of the stellar wind, these flows slow down and then stop at distances of  $\sim 6$  and  $\sim 4$  planetary radii from its center, forming a stationary envelope.
2. The planet and its envelope move in the gas of the stellar wind with a supersonic velocity resulting in a Mach number  $M = 2.14$ . Thus, the dynamic pressure of the stellar wind not only works toward the formation of the stationary envelope but also leads to the formation of a bow shock and contact discontinuity, which delimit the envelope. The wave has a complex double-peaked shape.
3. The head-on collision point found in the calculations is at the peak of the stream from the  $L_1$  point. The distance from

the planet to the head-on collision point, as projected to the stellar limb, is of  $\sim 4.5$  planetary radii, allowing us to explain the observed extent of the early ingress.

4. The heating of the planet envelope by the bow shock allows one to explain the fact that the eclipse, in the spectral bands where the early ingress has been observed, is two times deeper than the eclipse of the planet itself.

Summarizing our results, we found that by using the full gas dynamic simulations of the stellar wind interaction between WASP-12b and its host star, we have been able to obtain an alternative and self-consistent flow pattern allowing the explanation of the existing observational data.

This work was supported by the Basic Research Program of the Presidium of the Russian Academy of Sciences, Russian Foundation for Basic Research (projects 11-02-00076, 11-02-00479, 12-02-00047), Federal Targeted Program "Science and Science Education for Innovation in Russia 2009–2013." H.L. and D.B. acknowledge the support by the FWF NFN project S116 and the related FWF NFN subproject S116607-N16. Finally, D.B., L.F., V.S., and H.L. acknowledge support by the International Space Science Institute in Bern, Switzerland, and the ISSI team "Characterizing Stellar- and Exoplanetary Environments."

#### REFERENCES

- Baranov, V. B., & Krasnobaev, K. V. 1977, *Hydrodynamic Theory of a Cosmic Plasma* (Moscow: Nauka)
- Ben-Jaffel, L. 2007, *ApJL*, **671**, 61
- Bisikalo, D. V., Boyarchuk, A. A., Kaygorodov, P. V., & Kuznetsov, O. A. 2003, *ARep*, **47**, 809
- Bisikalo, D. V., & Fridman, A. M. 2008, *PhyU*, **51**, 551
- Boyarchuk, A. A., Bisikalo, D. V., Kuznetsov, O. A., & Chechetkin, V. M. 2002, *Mass Transfer in Close Binary Stars* (London: Taylor & Francis)
- Campo, C. J., Harrington, J., Hardy, R. A., et al. 2011, *ApJ*, **727**, 125
- Chan, T., Ingemyr, M., Winn, J. N., et al. 2011, *AJ*, **141**, 179
- Ekenbäck, A., Holmström, M., Wurz, P., et al. 2010, *ApJ*, **709**, 670
- Fossati, L., Bagnulo, S., Elmasli, A., et al. 2010a, *ApJ*, **720**, 872
- Fossati, L., Haswell, C. A., Froning, C. S., et al. 2010b, *ApJL*, **714**, 222
- Hebb, L., Collier-Cameron, A., Loeillet, B., et al. 2009, *ApJ*, **693**, 1920
- Ionov, D. E., Bisikalo, D. V., Kaygorodov, P. V., & Shematovich, V. I. 2012, in *IAU Symp. 282, From Interacting Binaries to Exoplanets: Essential Modeling Tools*, ed. M. T. Richards & I. Hubeny (Cambridge: Cambridge Univ. Press), **545**
- Koskinen, T., Yelle, R. V., Harris, M. J., & Lavvas, P. 2012, *Icar*, in press, <http://dx.doi.org/10.1016/j.icarus.2012.09.026>
- Lai, D., Helling, Ch., & van den Heuvel, E. P. J. 2010, *ApJ*, **721**, 923
- Lammer, H., Kislyakova, K. G., Holmström, M., Khodachenko, M. L., & Grießmeier, J.-M. 2011, *Ap&SS*, **335**, 9
- Li, S.-H., Miller, N., Lin, D. N. C., & Fortney, J. J. 2010, *Natur*, **463**, 1054
- Llama, J., Wood, K., Jardine, M., et al. 2011, *MNRAS*, **416**, L41
- Lubow, S. H., & Shu, F. H. 1975, *ApJ*, **198**, 383
- Murray-Clay, R. A., Chiang, E. I., & Murray, N. 2009, *ApJ*, **693**, 23
- Pringle, J. E., & Wade, R. A. 1985, *Interacting Binary Stars* (Cambridge: Cambridge Univ. Press)
- Savonije, G. J. 1979, *A&A*, **71**, 352
- Showman, A. P., & Guillot, T. 2002, *A&A*, **385**, 166
- Verigin, M., Slavin, J. A., Szabo, A., et al. 2003, *JGR*, **108**, 1323
- Vidal-Madjar, A., Désert, J.-M., Lecavelier des Etangs, A., et al. 2004, *ApJL*, **604**, 69
- Vidal-Madjar, A., Lecavelier des Etangs, A., Désert, J.-M., et al. 2003, *Natur*, **422**, 143
- Vidotto, A. A., Jardine, M., & Helling, Ch. 2010, *ApJL*, **722**, 168
- Vidotto, A. A., Jardine, M., & Helling, Ch. 2011, *MNRAS*, **414**, 1573
- Withbroe, G. L. 1988, *ApJ*, **325**, 442
- Yelle, R. 2004, *Icar*, **170**, 167
- Zhilkin, A. G., Bisikalo, D. V., & Boyarchuk, A. A. 2012, *PhyU*, **55**, 115